

PERFORMANCE OF ADOBE VAULTS STRENGTHENED WITH LC-TRM: AN EXPERIMENTAL APPROACH

Neda H. Sadeghi*, Daniel V. Oliveira*, Rui A. Silva*,
Nuno Mendes*, Mariana Correia**, Hamed Azizi-Bondarabadi*

* ISISE, University of Minho, Guimarães, Portugal
e-mails: neda.hsadeghi@gmail.com, danvco@civil.uminho.pt, ruisilva@civil.uminho.pt,
nunomendes@civil.uminho.pt, hamed.azizi@civil.uminho.pt

** Escola Superior Gallaecia, Vila Nova de Cerveira, Portugal
e-mail: marianacorreia@esg.pt

Keywords: Adobe vaults; Seismic assessment; Fiber-glass mesh; Strengthening; Failure mechanisms.

Abstract. *Due to the vulnerability of vaulted adobe buildings during the past earthquakes, it is crucial for such building typology to be evaluated in terms of seismic capacity. This paper deals with the seismic performance of historic vaulted adobe construction in adobe houses, typical from the city of Yazd, Iran. To this end, six 1:3 scaled adobe vaults were analyzed experimentally aiming at estimating their structural performance. The tests were performed in loading-unloading steps of increasing amplitude of an imposed vertical displacement at 30% of span. The tests were carried out in two unstrengthened and four strengthened adobe vaults. Vaults were strengthened with a low cost textile reinforced mortar (LC-TRM), where a low cost fiber-glass mesh is covered with an earth-based mortar. Two adobe vaults were strengthened at intrados and the other two at extrados. The experimental results show that the vaults behavior is enhanced due to the LC-TRM application, with respect to the unstrengthened vaults. A significant increase of the load carrying capacity and also an important improvement in ductility was evident. In addition, new failure mechanisms were observed for the strengthened vaults when compared with the formation of the typical four-hinge mechanism of unstrengthened vaults.*

1 INTRODUCTION

Adobe vaults arising from thousands of years of development and refinement are outside the scope of the majority of available researches. Hence, stability and safety of this spectacularly complex roofing type system during an earthquake are considerably unknown. Adobe vaults are generally characterized by weak and brittle materials, weak connections and excessive weight so that their collapse had become a major cause of human fatalities (e.g. failure of vaulted adobe buildings after the 2003 Bam earthquake) [1-6]. Based on the literature, most of the seismic studies on adobe constructions are addressed to case studies [2, 7-9], mechanical behavior of adobe units and prisms [10-12], adobe walls [13-15] and scaled adobe structures with wooden pitched or flat roofs [16-19]. Moreover, the majority of researches in the field of masonry vaulted structures is related to stone and brick vaults [20-25]. In spite of the demonstrated adobe vaults vulnerability during past earthquakes, only a limited number of studies on the seismic behavior of adobe vaulted structures can be found in literature. In PUCP, Peru, two vaulted models, one unreinforced and the other fully reinforced, were subjected to seismic simulation tests and the results showed that the unreinforced specimen was very vulnerable, but the fully reinforced vaults, on the contrary, performed well [26]. Sathiparan and Meguro [27] also evaluated the seismic behavior of models of adobe vaulted houses using different retrofitting methods. There is also a few

number of field surveys based on case studies, such as adobe vaulted buildings performance in Bam earthquake [1, 4].

Adobe vault architectures were originated and developed in the Middle East, one of the high seismic prone regions of the world, and date back to more than 3000 years ago [28]. Based on archaeological excavations, it can be stated that arches and vaults were widely and diversely employed in the ancient Middle-East, from southern Egypt to western Persia [29]. Iran, located on the Alpine-Himalayan earthquake belt as one of the most seismically active areas of the world, has a vast number of vernacular adobe constructions. The city of Yazd in the central part of the Iranian plateau has an integrated adobe residential architecture. On the other hand, Yazd is a region with a relatively high seismic hazard, having a design peak ground acceleration of 0.25g for a return period of 475 years [30]. The seismicity of Yazd, in addition to the well-known seismic vulnerability of vaulted adobe construction, gives rise to an urgent need for evaluating the seismic performance of vaulted adobe houses located in Yazd. For achieving this purpose, a reference vault, which is geometrically representative of adobe vaults in the adobe houses of Yazd [31], was selected.

In order to evaluate the behavior of aforementioned adobe vaults, a combined experimental-numerical research project was carried out at University of Minho, see also [31, 32]. This paper reports and discusses the main results of the experimental work, aiming at estimating the structural performance of adobe vaults, before and after strengthening.

2 BEHAVIOR AND FAILURE MECHANISM OF MASONRY VAULTS

Wide reviews of historical studies on masonry arches and vaults can be found in Benvenuto [33], Heyman [34], and Carbone, Fiore [35], among others. Heyman clearly formalized some hypotheses in order to form the basis for the calculation of the arches and vaults in the past centuries [36], by assuming that masonry has zero tensile strength and that the masonry arch is kept in compression. The concept of the thrust line is used to visualize the forces resultant within the arched and vaulted structures. In such a way that, arch and vault are assumed safe when the thrust line can be drawn totally inside the arch and vault thickness. Cracks develop at the arch and vault cross-section due to the movement of trust lines outward the central core at a given cross section. Moreover, increasing the load causes to deepen the cracks, which lead to the formation of hinges at the intrados or extrados of the arches and vaults. The development of a hinge-based mechanism in arched and vaulted structures causes their failure. It should be noted that four hinges are necessary for masonry arches and vaults loaded asymmetrically to form a failure mechanism.

As mentioned, masonry vaulted buildings, especially weak structures such as adobe ones, are vulnerable to earthquakes, see Figure 1(a). To study the seismic behavior of arched and vaulted structures, Oppenheim [37] introduced an analytical model describing the masonry arch as a single degree of freedom three-bar (four-hinge) mechanism, see Figure 1(b).

In order to analyze the seismic performance of masonry vaults experimentally, a test procedure that contributes to understanding the structural performance of vaults is the application of a concentrated vertical load at one-third or quarter vault span. The additional point loads have a thrusting nature and, due to their action, move the trust line outward the vault cross-section and develop four hinges that lead to collapse [38], as shown in Figure 1(c). It is noteworthy to mention that the typical failure mechanism of masonry vaults submitted to concentrated vertical loads and under the seismic load are approximately similar. In addition, testing setups for static load application are much easier, cheaper, faster and more available than for dynamic loading application. Due to these facts, this typology of static tests was adopted in the experimental program of this research work.

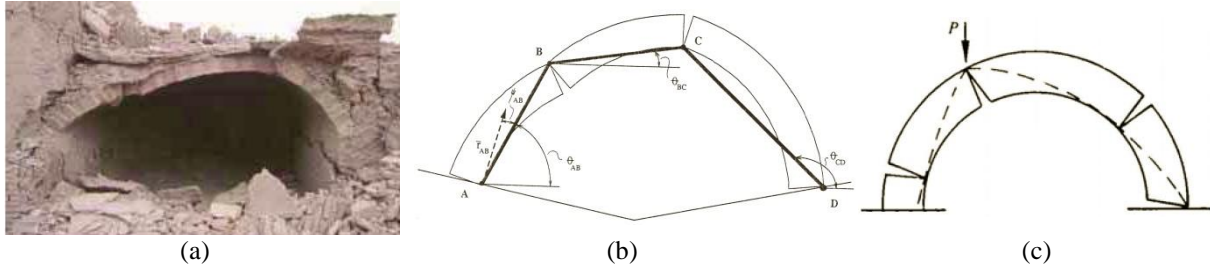


Figure 1: Failure mechanism of vaults: (a) adobe vault after Bam earthquake (2003); (b) masonry vault under seismic load [37]; (c) masonry vault subjected to a concentrated load at quarter-span

3 DESCRIPTION OF THE VAULT MODEL

3.1 Geometry

Most of the adobe buildings in Yazd have vaulted adobe roofs, where the majority of the surveyed vaults have segmental shape and different constructive solutions can be found over them. Some vaults are without fill, while in others the space above the vaults is fully filled with soil or with adobe spandrel walls with small vaults on top (named “konou” in Persian architectural literature) in order to create the flat roofs above.

In order to better understand the vaulted adobe structure of the houses in Yazd, vaults of “Talar” space were selected due to its presence in most of the traditional houses. Moreover, these vaults often have the largest span among all the house’s vaults. A geometric study of the vaulted constructions under study was previously performed in order to define the reference vaults combinations as representative of the samples [31]. In this paper, the main vault of the aforementioned reference vaults combination, which is dominant in the studied samples, has been selected in order to be analyzed experimentally. The span length of this segmental vault is 5700 mm and its rise is 1300 mm, with a thickness equal to 250 mm.

Aiming at replicating the mentioned adobe vaults, an experimental work has been carried out on six reduced one-third scale adobe vaults with 1900 mm span, 430 mm rise and 90 mm thickness (for the sake of construction simplicity, the thickness of vaults has been assumed 90 mm instead of 83 mm), while the width of adobe vaults was taken as 450 mm. The geometry adopted for the adobe vaults is illustrated in Figure 2. In order to keep the construction process and the test setup as simple as possible, the vault has been considered without infill. Furthermore, the influence of the dead load of soil or spandrel walls and vaults applied at extrados was not considered, as it can be studied numerically after calibration of an adequate numerical model.

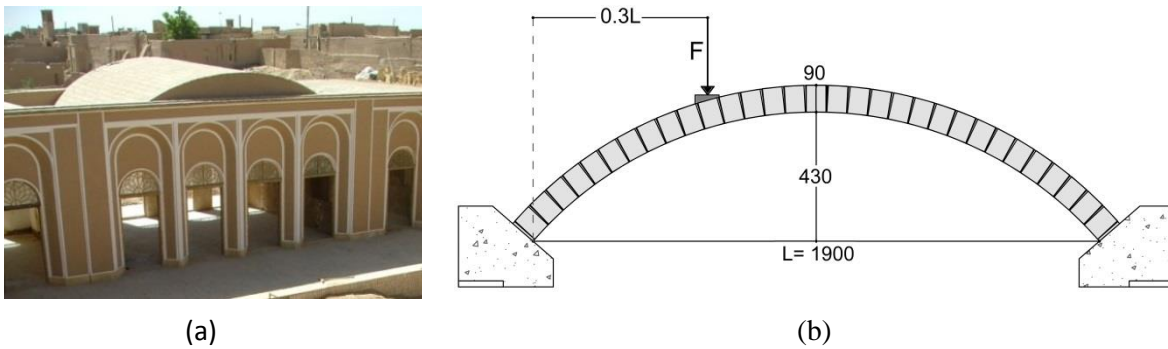


Figure 2: (a) Adobe house in Yazd; (b) Adopted vault geometry and load arrangement

3.2 Procedure for construction and strengthening

With the purpose of building the adobe vaults and prisms, about 4000 one-third scaled adobe units, with dimensions 90 mm × 650 mm × 20 mm, were produced at the laboratory (see Figure 3(a) and (b)). In order to produce adobe vaults as representative as possible as those belonging to historic adobe houses from Yazd, the vaults were built using handmade adobes with mechanical properties similar to those of adobes applied in historic constructions of Yazd. To this end and after testing adobe units and prisms of different mixtures, the composition of the adobes was set as 80% of sieved soil ($\leq 5\text{mm}$), 10 % of kaolin clay, 10% of cement (in weight), whereas water was added according to the workability defined by the mason as required to mold the adobes. The bed joint mortar consisted of a mixture of sieved soil ($\leq 2\text{mm}$) and clay with the following weight percentage, respectively: 87% and 13%. The water solids ratio of mortars is about 0.39.

All six vaults consisted of 15 circumferential courses with about 31-32 adobes in each course. This type of construction, where units are laid vertically to the circumferential courses, was dominant in countries such as Iran and Egypt. Originally, these vaulted roofs were built without requiring formwork or support during construction, since the vaults were constituted by several inclined arches laid together [3]. In the current experimental work, due to the need to simplify the construction procedure and to the absence of a skilled mason knowing how to build without formwork, the vaults were built from vertical courses over a wooden mold. Two concrete blocks were fixed to the strong floor at both sides as rigid supports. The construction of each vault took place during two days, while the wooden mold was carefully removed one week after construction. Figure 3(c) and (d) illustrate the construction of one vault.



Figure 3: Production of the adobe units and construction of the vaults: (a) molding of adobes; (b) demolding and drying/curing of adobes; (c) construction of a vault; (d) vault after construction

Three different sets of vaults were studied in the experimental program. The first set was composed of two vaults without any strengthening (UN1 and UN2). The other two sets of vaults were strengthened with a low cost textile reinforced mortar (LC-TRM), where fiber-glass mesh is covered with a mortar composed of soil, lime and clay with the weight percentage of 80%, 10% and 10% respectively. The water solids ratio of mortars is about 0.39. Two adobe vaults were strengthened at intrados (SI1 and SI2) and the other two at extrados (SE1 and SE2). Figure 4(a) and (b) illustrate both types of strengthening.

Detachment of the strengthening layer from the masonry can be one of the major causes of failure for intrados strengthening [25]. In the case of adobe vaults strengthened at intrados, in order to mitigate this problem, 4 spike anchors were applied in each vault, at 1/8 and 3/8 of

span length on the loaded half-side, two fixing rods were used in each alignment at 1/4 and 3/4 of the vault width, see also Figure 4(c).

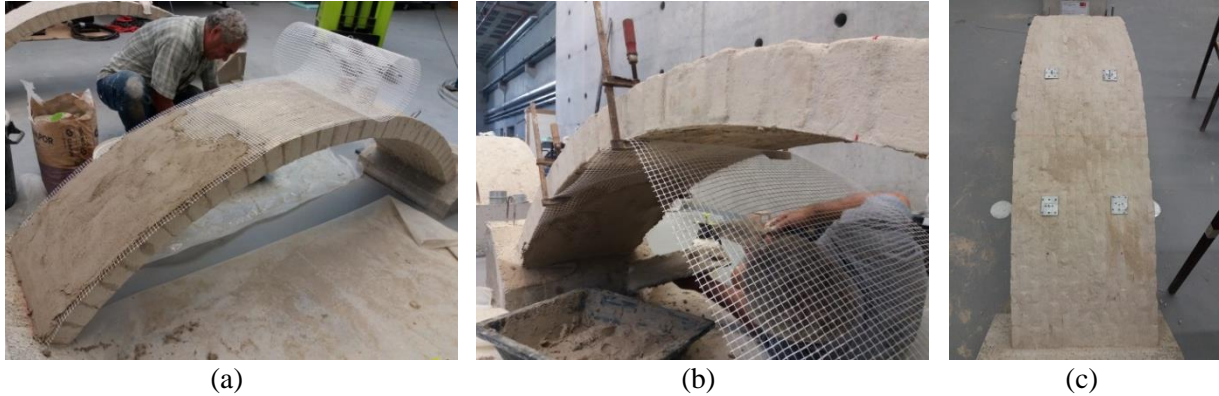


Figure 4: Strengthening of adobe vaults with LC-TRM: (a) at extrados; (b) at intrados; (c) 4 spike anchors applied to vaults strengthened at intrados

4 EXPERIMENTAL PROGRAM

4.1 Materials characterization

Before building the adobe vaults, comprehensive material tests were conducted to assess the mechanical properties of the materials. Adobe prisms and cylindrical specimens of the adobe mixture were tested in order to obtain their compressive strength and Young modulus. Specimens of the bed joint and strengthening mortars were tested to evaluate their compression and flexural strengths. The tensile strength and elastic modulus of the fiber-glass mesh used for strengthening the adobe vaults were also characterized for both longitudinal (x) and transversal (y) directions. Average values of the mechanical properties obtained from these tests are presented in Table 1.

Table 1: Average mechanical properties of the adobe masonry materials and strengthening materials

Materials	Dimensions	Compressive strength	Tensile strength	Young modulus	Flexural strength	Density
Adobe masonry (prisms)	220×100×140 [mm]	0.65 [MPa]	-	480 [MPa]	-	1460 [kg/m ³]
Adobe (cylinders)	Ø100×200 [mm]	1.2 [MPa]	-	790 [MPa]	-	1500 [kg/m ³]
Bed joint mortar (prisms)	160×160×40 [mm]	0.74 [MPa]	-	-	0.26 [MPa]	1440 [kg/m ³]
Strengthening mortar (prisms)	160×160×40 [mm]	0.47 [MPa]	-	-	0.19 [MPa]	1360 [kg/m ³]
Strengthening mortar (cylinders)	Ø100×200 [mm]	0.31 [MPa]	-	403	-	1340 [kg/m ³]
Fiber-glass mesh	100×400 [mm]	-	16.8 [kN/m] (x) 12.2 [kN/m] (y)	980 [kN/m] (x) 626 [kN/m] (y)	-	105.3 [g/m ²]

4.2 Test setup

Tests were performed in loading-unloading steps of increasing amplitude of an imposed vertical displacement applied at about 30% of the vault span (defined by the position of the reaction frame), as depicted in Figure 5. The amplitude varied between 0.48 mm and 42 mm, while the displacement rate was of 10-15 µm/s and 10-50 µm/s, respectively for loading and

unloading. It should be noted that the loading-unloading rates were increased as the amplitude increased, in order to keep the duration of the last steps shorter than 60 min.

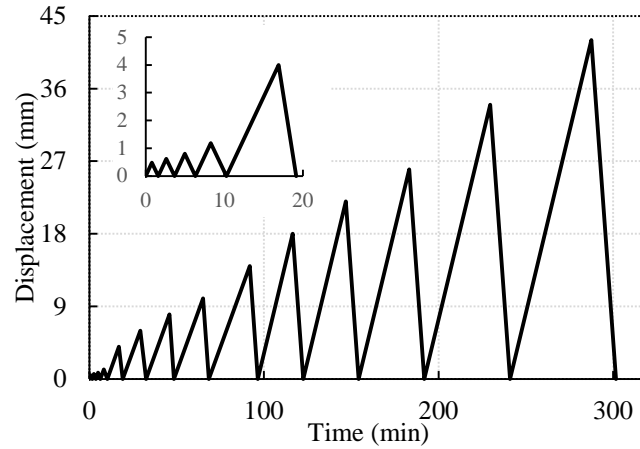


Figure 5: Loading-unloading stepwise profile applied to the vaults

The load was distributed transversally via a rigid steel beam, which was placed over a timber element shaped according to the curvature of the vault. The rigid beam was perpendicular to the span of the vaults. In order to improve the initial stress state of the vaults, an additional load of 0.5 kN, composed of two bags of 25kg mass, was applied at the center of the vaults. The load was recorded by means of a 10 kN load cell equipping the loading actuator. Eight linear variable differential transducers (LVDTs) were placed at defined locations, aiming at monitoring the vault deflection. Two LVDTs were applied at midspan and four LVDTs were located at 30% of the vault span from both supports. The other two LVDTs were placed at the springers of the vault to control possible displacements at the supports.

In the case of vaults UN1 and UN2, tests were stopped before complete failure, which made possible to strengthen them and to perform two more tests, not reported here. The other four vaults were tested up to failure. In order to minimize possible damage to test equipment and spreading of debris, a few blocks were placed beneath the vaults (at an acceptable distance), as to control the possible displacements of the collapsed parts.

5 RESULTS OF TESTS

During the tests, a visual inspection of the vaults was continuously performed to register the cracking pattern as well as possible detachment of the LC-TRM, hinges location and failure pattern of the vaults. Some initial minor cracks due to shrinkage were observed in the vaults before the tests.

The relation between load and corresponding vertical displacement beneath the load application point is depicted in Figure 6, while the peak load, maximum displacement and initial stiffness of each vault are listed in Table 2. Different ductility behaviors were observed between the three groups of vaults. In the following sections, the results of the experimental tests carried out on the vaults are grouped according to the strengthening strategy followed.

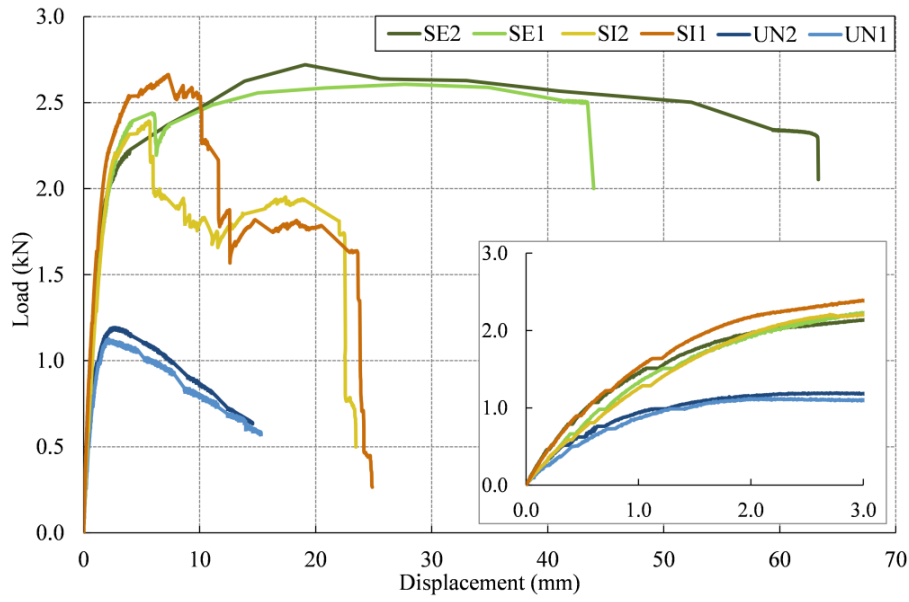


Figure 6: Envelope of load-displacement curves at the load point

Table 2: Results of the tests performed on the vaults

Vault	Peak load		80% of Peak load		Max. displ.		Initial stiffness (kN/mm)
	F (kN)	Displ. (mm)	F (kN)	Displ. (mm)	F (kN)	Displ. (mm)	
UN1	1.13	2.13	0.84	8.67	0.57	15.3	1.42
UN2	1.19	2.70	0.95	8.27	0.63	14.57	1.57
SE1	2.61	27.67	*	*	2.49	43.44	1.70
SE2	2.72	19.10	*	*	2.28	63.29	2.46
SI 1	2.66	7.31	1.84	11.63	1.62	23.63	2.31
SI 2	2.39	5.61	1.89	7.96	1.57	22.52	1.67

*: collapse occurred before reaching this value

5.1 Unstrengthened adobe vaults

The test procedure of the two unstrengthened vaults included eight loading-unloading steps. Experimental results of these adobe vaults show a similar structural behavior. Absence of ductility with the formation of four-hinge mechanisms was observed in these tests. The block mechanism was activated after the vaults reached the maximum load at the 5th step of the test. The typical behavior of the unstrengthened vaults is depicted in Figure 7, which contains the deformed shape of vaults and some views of the hinges.

Based on the visual inspection and LVDTs results, it can be stated that the vaults moved downward near the load and upward at 30% of vault span on the other side. In the case of these vaults, hinges happened when the line of thrust passed the edge of the vault. Hinges were developed in the place of the applied load (intrados), at about the quarter span of the vault at the symmetric side of the loaded side (extrados) and at the both vault springings, near the supports, which is shown in Figure 7. Note that the tests of unstrengthened adobe vaults were stopped before their complete failure.

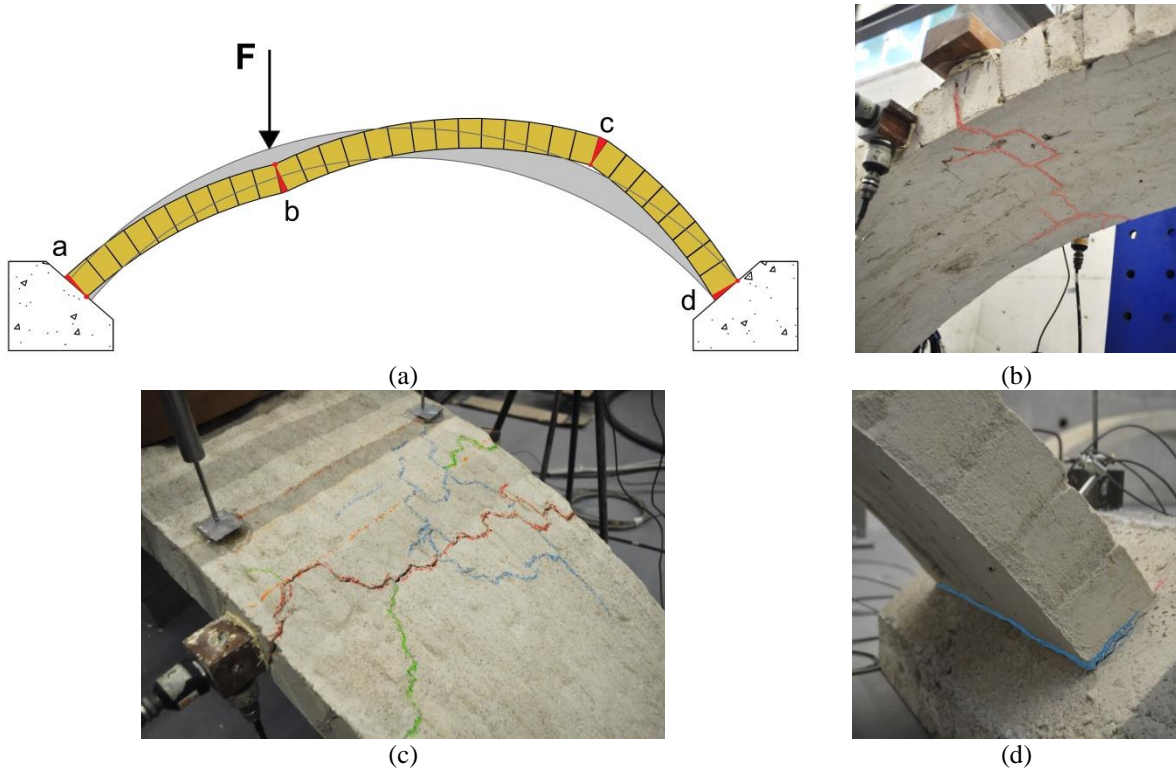


Figure 7: Unstrengthened vaults: (a) four-hinge failure mechanism developed; (b) hinge b; (c) hinge c; (d) hinge d

5.2 Adobe vaults strengthened at extrados

Testing of the two strengthened vaults at extrados, SE1 and SE2, included twelve and fourteen loading-unloading steps, respectively. These vaults presented different behavior and collapse patterns, as shown in Figure 8(a). This type of strengthening prevents the opening of hinges at the extrados. At the location opposite to the load application, a distributed crack pattern appeared and kept spreading towards the support; see Figure 8(b). In fact, the LC-TRM prevented the fourth hinge to occur. Instead, the vaults developed three hinges and one additional “release” [39] as presented in Figure 8(c). The position of the three hinges is similar with the unstrengthened vaults case. Hinges developed at the load application cross-section and at both vault springings. Figure 8(d) presents the deep crack under the load at the intrados of the vault.

An increment in peak load and a huge increase of maximum displacement were observed. A very important feature observed in these tests was the long post-peak branch that shows improvement in displacement ductility when compared to the unstrengthened vaults. In addition, an increase of initial stiffness was also visible.

5.3 Adobe vaults strengthened at intrados

Testing of the two strengthened vaults at intrados (SI1 and SI2) included ten loading-unloading steps. In these tests, the vaults presented different behavior and patterns of collapse with respect to the results obtained for the two previous groups. Intrados strengthening prevents the opening of any hinge at the intrados. As before, LC-TRM prevents the fourth hinge to occur and only three hinges and one additional “release” were developed. The three hinges developed at about quarter-span on the symmetric side with respect to load application side and at both vault springings, see Figure 9(a).

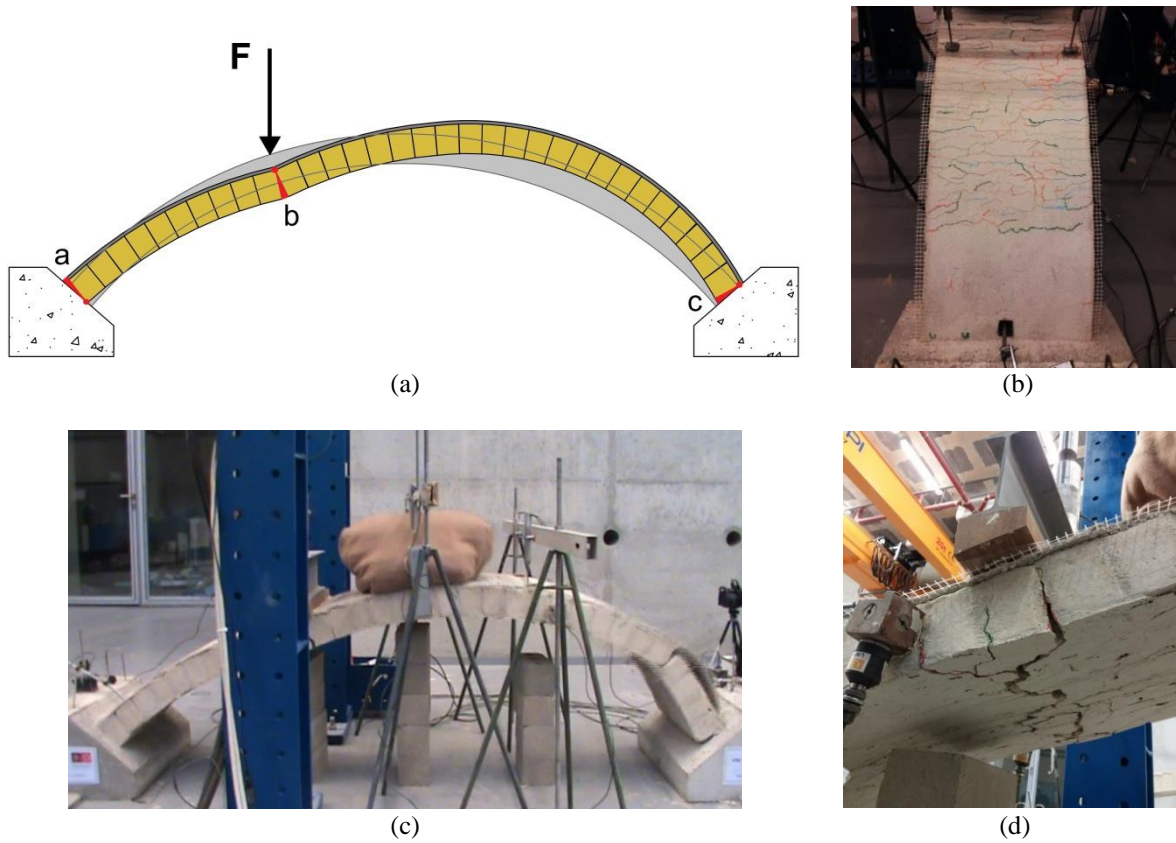


Figure 8: Strengthened vaults at extrados: (a) three-hinges failure mechanism; (b) small cracks at the place opposite to the load application point; (c) vaults near to complete collapse with three hinges and one additional “release”; (d) hinge b

In both SI1 and SI2 vaults, failure occurred due to the detachment of the LC-TRM from the substrate, close to the load application cross-section. However, the spike anchors applied to fix the strengthening postponed the full detachment of this layer. The load drops visible in the load-displacement curves were due to progressive detachment of the LC-TRM, see Figure 6 and Figure 9.

A considerable increment in peak load and maximum displacement were observed, i.e. the post-peak branches show improvement in ductility. In addition, an increase in their initial stiffness was observed when compared to the unstrengthened vaults.

6 MAIN CONCLUSIONS

This paper deals with the seismic performance of historic vaulted adobe construction in adobe houses typical from the city of Yazd, Iran. To this end, the experimental performance of six one-third scaled segmental adobe vaults, unstrengthened and strengthened with LC-TRM has been presented and discussed in this paper.

The experimental results on the adobe vaults show that strengthening with LC-TRM provides an enhancement in terms of initial stiffness, load capacity and displacement capacity with respect to the unstrengthened vaults. However, the degree of improvement depends on the strengthening strategy followed.

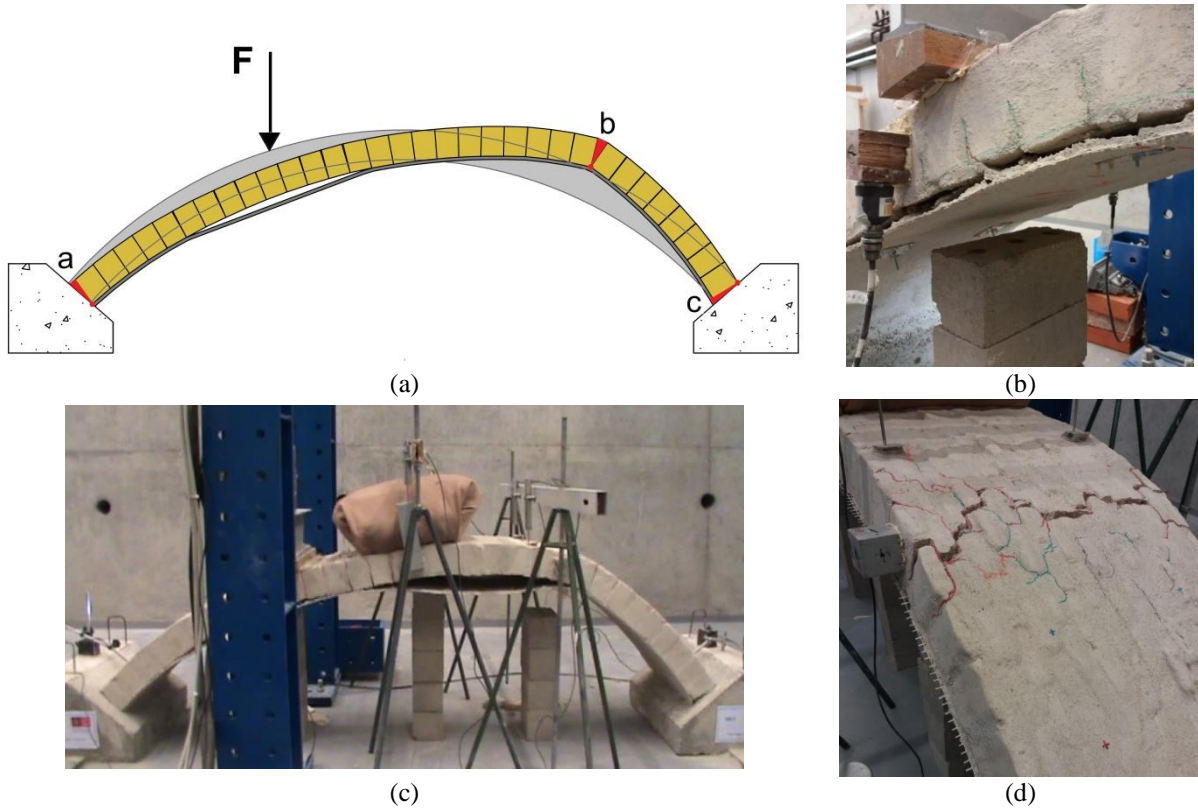


Figure 9: Strengthened vaults at intrados: (a) three-hinges failure mechanism; (b) detachment of LC-TRM at the load location; (c) vaults near to complete collapse with three hinges and one additional “release”; (d) hinge b

In the experiments without strengthening, the formation of a typical four-hinge mechanism and absence of ductility were observed, while the application of LC-TRM prevented the formation of four hinges. In other words, the strengthened adobe vaults developed only three hinges and one additional “release”. The experimental results show that strengthening applied at the extrados provides a slightly higher increment in terms of load capacity, but much more deformation capacity prior to failure when compared with the intrados strengthening.

In order to provide a general overview of the three sets of adobe vaults, Table 3 summarizes the quantitative data regarding the peak load and maximum displacement increase achieved by the application of LC-TRM strengthening. If one assumes that conventional collapse occurs for a post-peak load equal to 80% of the peak load, it can be stated that the vaults are near its collapse limit state.

Table 3: Experimental results concerning the maximum load, strength increase, corresponding displacement for 80% of peak load and displacement increase

Vault	Peak load (kN)	Strength increase	Displacement at 80% of peak load (mm)	Displacement increase
UN1	1.13	-	8.67	-
UN2	1.19	-	8.27	-
SE1	2.61	+125%	43.44 ^(*)	+413%
SE2	2.72	+134%	63.29 ^(*)	+647%
SI 1	2.66	+129%	11.63	+37%
SI 2	2.39	+106%	7.96	-6%

^(*) Maximum displacement (vaults SE1 and SE2 collapsed before reaching 80% of peak load).

Finally, the experimental results presented in this paper can provide an important database for the calibration of analytical and advanced numerical models for the simulation of the structural performance of adobe vaults.

ACKNOWLEDGMENTS

This work was partly financed by FEDER funds through the Competitiveness Operational Program - COMPETE and by national funds through FCT – Foundation for Science and Technology within the scope of projects POCI-01-0145-FEDER-007633 and POCI-01-0145-FEDER-016737 (PTDC/ECM-EST/2777/2014).

REFERENCES

- [1] Mahdi, T. *Performance of traditional arches and domes in recent Iranian earthquakes*. in *Earthquakes 13th World Conf. on Earthquake Engineering*. 2004.
- [2] Maheri, M.R., Naeim, F., and Mehrain, M., *Performance of Adobe Residential Buildings in the 2003 Bam, Iran, Earthquake*. *Earthquake Spectra*, 2005. **21**(S1): p. 337-344.
- [3] Minke, G., *Building with Earth: Design and Technology of a Sustainable Architecture*. 2006: Birkhäuser Basel.
- [4] Maïni, S., *The French contribution to the reconstruction of Bam and its citadel : diagnosis of damages to vaulted structures Arg-e Bam and Bam town, Iran* . 2004.
- [5] Zahrai, S.M. and Heidarzadeh, M. *Seismic Performance of Existing Buildings During the 2003 Bam Earthquake*. in *Proceedings of the 13th World Conference on Earthquake Engineering, Vancouver, Canada, Paper*. 2004.
- [6] Ashtiany, M., *Preliminary Observations on the Bam, Iran, Earthquake of Dec. 26, 2003*, 2004, Earthquake Engineering Research Institute (EERI).
- [7] Tarque, N., Crowley, H., Pinho, R., and Varum, H., *Displacement-Based Fragility Curves for Seismic Assessment of Adobe Buildings in Cusco, Peru*. *Earthquake Spectra*, 2012. **28**(2): p. 759-794.
- [8] Dowling, D., *Adobe housing in El Salvador: Earthquake performance and seismic improvement*. Geological society of America, 2004: p. 281-300.
- [9] Tolles, E.L., Webster, F.A., Crosby, A., and Kimbro, E.E., *Survey of Damage to Historic Adobe Buildings after the January 1994 Northridge Earthquake*, 1996, Getty Conservation Institute.
- [10] Silveira, D., Varum, H., Costa, A., Martins, T., Pereira, H., and Almeida, J., *Mechanical properties of adobe bricks in ancient constructions*. *Construction and Building Materials*, 2012. **28**(1): p. 36-44.
- [11] Silveira, D., Varum, H., and Costa, A., *Influence of the testing procedures in the mechanical characterization of adobe bricks*. *Construction and Building Materials*, 2013. **40**(0): p. 719-728.
- [12] Eslami, A., Ronagh, H.R., Mahini, S.S., and Morshed, R., *Experimental investigation and nonlinear FE analysis of historical masonry buildings – A case study*. *Construction and Building Materials*, 2012. **35**(0): p. 251-260.
- [13] Bossio, S., Blondet, M., and Rihal, S., *Seismic Behavior and Shaking Direction Influence on Adobe Wall Structures Reinforced with Geogrid*. *Earthquake Spectra*, 2013. **29**(1): p. 59-84.
- [14] Figueiredo, A., Varum, H., Costa, A., Silveira, D., and Oliveira, C., *Seismic retrofitting solution of an adobe masonry wall*. *Materials and Structures*, 2013. **46**(1-2): p. 203-219.
- [15] Varum, H., et al., *Structural Behaviour and Retrofitting of Adobe Masonry Buildings*, in *Structural Rehabilitation of Old Buildings*, A. Costa, J.M. Guedes, and H. Varum, Editors. 2014, Springer Berlin Heidelberg. p. 37-75.
- [16] Illampas, R., *Experimental and computational investigation of the structural response of adobe structures*, in *Department of civil and environmental engineering* 2013, University of Cyprus.
- [17] Tarque, N., *Numerical modelling of the seismic behaviour of adobe buildings*, in *ROSE School, Istituto di Studi Superiori di Pavia* 2011, Università degli Studi di Pavia: Pavia, Italy.

- [18] Tolles, E.L., Kimbro, E.E., Webster, F.A., and Ginell, W.S., *Seismic Stabilization of Historic Adobe Structures*: , in *Final Report of the Getty Adobe Project*2000, Getty Conservation Institute: Los Angeles.
- [19] Blondet, M., Vargas Neumann, J., Velásquez, J., and Tarque, N. *Experimental study of synthetic mesh reinforcement of historical adobe buildings*. in *SAHC2006. Structural Analysis of Historical Constructions*. 2006. New Delhi, India.
- [20] Como, M., *Statics of historic masonry constructions*. Vol. 1. 2012: Springer.
- [21] UNIPD, U.o.P. *NIKER*. Deliverable 5.1- Specification for laboratory specimens and testing strategies on floors and vaults., 2013.
- [22] Giardina, G., *Studio sul comportamento sismico di archi in muratura*. 2006, Brescia, Italy: Università degli Studi di Brescia.
- [23] Taranu, N., Oprisan, G., Budescu, M., Taranu, G., and Bejan, L. *Improving structural response of masonry vaults strengthened with polymeric textile composite strips*. in *3rd WSEAS international conference on Engineering mechanics, structures, engineering geology*. 2010. World Scientific and Engineering Academy and Society (WSEAS).
- [24] Girardello, P., *Rinforzo di volte in muratura con materiali compositi innovativi*, 2013, Università' Degli Studi di Brescia.
- [25] Oliveira, D.V., Basilio, I., and Lourenço, P.B., *Experimental behavior of FRP strengthened masonry arches*. *Journal of Composites for Construction*, 2010. **14**(3): p. 312-322.
- [26] Torrealva, D., Vargas Neumann, J., and Blondet, M. *Earthquake resistant design criteria and testing of adobe buildings at Pontificia Universidad Catolica del Peru*. in *Getty Seismic Adobe Project 2006 Colloquium*. 2006. Los Angeles, CA: Getty Conservation Institute
- [27] Sathiparan, N. and Meguro, K., *Strengthening of adobe houses with arch roofs using tie-bars and polypropylene band mesh*. *Construction and Building Materials*, 2015. **82**: p. 360-375.
- [28] Norton, J., *Woodless Construction: Unstabilised earth brick vault and dome roofing without formwork*. 1997.
- [29] Van Beek, G.W., *Arches and vaults in the ancient Near East*. *Scientific American*, 1987. **257**(1): p. 78-85.
- [30] USGS, U.S.G.S. 2014 2014; Available from: <http://pubs.usgs.gov/>.
- [31] Sadeghi, N., Oliveira, D.V., Correia, M., Azizi-Bondarabadi, H., and Orduña, A. *Numerical study on the seismic performance of adobe vaulted architecture: A case study from Iran*. in *International RILEM Conference on Materials, Systems and Structures in Civil Engineering, Conference segment on Historical Masonry*. 2016. Lyngby, Denmark.
- [32] Sadeghi, N., Oliveira, D.V., Correia, M., Azizi-Bondarabadi, H., and Orduña, A., *Seismic safety assessment of adobe vaulted architecture in Iran*, in *7th International Conference on Seismology and Earthquake Engineering*2015: Tehran, Iran.
- [33] Benvenuto, E., *La scienza delle costruzioni e il suo sviluppo storico*, Sansoni, Firenze, Italy. 1981.
- [34] Heyman, J., *The masonry arch*. 1982, New York: Ellis horwood
- [35] Carbone, I.V., Fiore, A., and Pistone, G., *Le costruzioni in muratura*. Hoepli, Milano, 2001.
- [36] Nobile, L. and Bartolomeo, V., *Methods for the Assessment of Historical Masonry Arches*.
- [37] Oppenheim, I.J., *The masonry arch as a four-link mechanism under base motion*. *Earthquake engineering & structural dynamics*, 1992. **21**(11): p. 1005-1017.
- [38] DeJong, M.J., *Seismic assessment strategies for masonry structures*, 2009, Massachusetts Institute of Technology.
- [39] Basílio, I., *Strengthening of arched masonry structures with composite materials*, in *Civil Engineering*2007, University of Minho: Guimaraes, Portugal.